Journal of Materials Science and Engineering A 12 (1-3) (2022) 1-12
doi: 10.17265/2161-6213/2022.1-3.001

Residual Stress Measurement Techniques for Additive Manufacturing Applications

Adi Ben-Artzy[1], Kahraman Demir[2], Jack Peterson[3], Stuart Maloy[4], Grace X. Gu[2] and Peter Hosemann[3,4]

1. Ben-Gurion university, PO Box 653, Beer-Sheva 84105, Israel

2. Department of Mechanical Engineering, University of California Berkeley, Berkeley, CA 94720, USA

3. Department of Nuclear Engineering, University of California Berkeley, Berkeley,CA 94720, USA

4. Lawrence Berkeley National Laboratory, Material Science Division, Berkeley, CA 94720, USA

Abstract: RSs (Residual stress) in engineering components can lead to dimensional instability, distortion during life cycle or in some cases catastrophic failure. RSs in AM (additive manufacturing) parts are a consequent of thermal expansion during heating, thermal contraction during solidification of each laser pass, and volume change due to phase transformations. Currently, most RS measurement techniques are destructive or semi-DT (destructive tests) based on releasing the RS by drilling or slitting the sample while X-ray or neutron diffraction techniques are considered as nondestructive techniques but require the use of powerful beams and slicing a small sample of the detected part. In this paper, a novel nondestructive RS measuring technique is presented, using fs (Femto-Second) laser trenching up to 250 μm depth. The fs-laser trenching relaxes surface stresses violating the stress balance that is measured by a bidirectional SG (strain gauge). In this work, RSs induced in low carbon steel samples using an IPG Photonics YLR500-AC-Y14 500 W YAG laser (simulating the last pass of SLM) were directly measured by proposed method. The results show the precision and accuracy of the fs-laser trenching and SG technique, that can be applied to evaluate RS in wrought and cast metals as well. This novel method still needs to be validated and be supported by a model.

Key words: AM, RS, fs laser, SG, laser.

1. Introduction

AM (additive manufacturing) of metals, is a popular prototyping and manufacturing technique which enables the production of geometrically complex parts using common or unique metals in a relatively short time. The raw material for metal AM can be in the form of powders, as used in PBF (powder bed fusion) processes including SLS (Selective Laser Sintering), SLM (selective laser melting), and LMD (laser metal deposition). Alternatively, wire can also be used as in WLMD (Wire Laser Metal Deposition) and WAAM (wire arc additive manufacturing) using a welding robot [1]. The power sources are usually lasers or electron beams. Other less common techniques use foils as metal source and friction as the energy input source for the consolidation of the metals. Most AM techniques involve melting and solidification of the added materials. The added metal is heated by the heat source up to and above the melting point followed by the solidification stage of the melted pool as the heat source proceeds to another area. The solidification is usually rapid due to the small volume of the melted pool in comparison to the much larger base metal surrounding it.

RSs (residual stresses) in AM processes are a consequence of three mechanisms: contraction tensile stresses due to volume change during the heating process [2] and contraction tensile stresses that appear during the solidification stage. Other stresses are created in some metals and alloys due to volume change as a result of phase transformation. Temperature gradients that induce non-uniform

Corresponding author: A. Ben-Artzy, Dr., research field: additive manufacturing.

thermal expansions and contractions surrounding the affected zone will result in additional stresses, while the latter mechanism tends to shrink the material because of its thermal contraction [3]. If the RS exceeds the bonding strength between layers, it might result in delamination, which depends on the scanning strategy [4]. RSs are destined to coalesce or vanish according to the build strategy, metal composition and other AM parameters. Fig. 1 demonstrates the state of stresses in the AM part due to the heating, melting and solidification of the part under the laser work.

There are numerous efforts invested in minimizing RS in AM. Preheating the substrate, heating the metal powder or the vicinity of melted pool by a second laser is done in order to decrease the temperature gradient [5]. It has been shown that using a multi-beam strategy in SLM allows for a significant RS reduction. The orientation of the scan vectors was found effective to AM layers delamination caused by RS [4]. They have determined the minimum and maximum electron beam scanning speed to minimize thermal stresses during melting and cooling steps, respectively. Most RS measurement techniques are destructive. Nondestructive methods include X-ray or neutron diffraction to measure peak width changes which are considered indirect measurements. Other techniques categorized as relaxation methods (destructive methods) include cutting or drilling the surface of interest causing a change in the balance of stresses, which results in a visible or measurable change on the surface [6]. A DT (Destructive Test) RS measuring technique for AM is demonstrated in Fig. 2 where the tensile stresses are released by EDM (ELECTRONICA Ultracut F2) wire cutting the AM part in the longitudinal direction, so the RS can be measured directly and can be associated with the AM build parameters and strategy [7].

RS measuring techniques are categorized by destructiveness as can be seen in Fig. 3a. Additionally, NDT (nondestructive test) techniques are compared through their resolution and penetration depth (Fig. 3b). X-ray and neutron diffractions are in the range of 100 μm resolution while neutrons penetrate three orders deeper than X-ray [8]. Since the penetration of XRD is limited, the inspected part needs to be cut in order to evaluate RS in the bulk area. This way the NDT X-ray technique is practically converted to a DT technique [3].

The contour method determines RS by cutting the specimen and measuring the deformation due to the released RS. The measurements are used to calculate the RS using a finite element model of the sample [9].

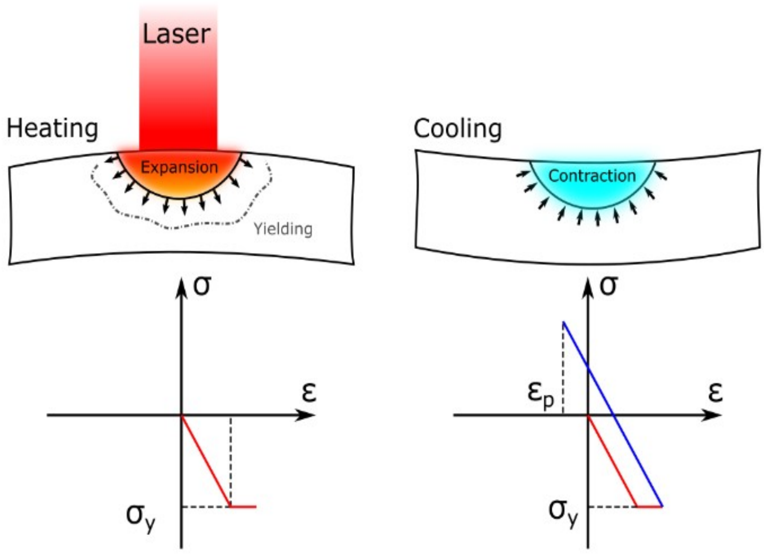

Fig. 1 Stresses state of RSs in AM.

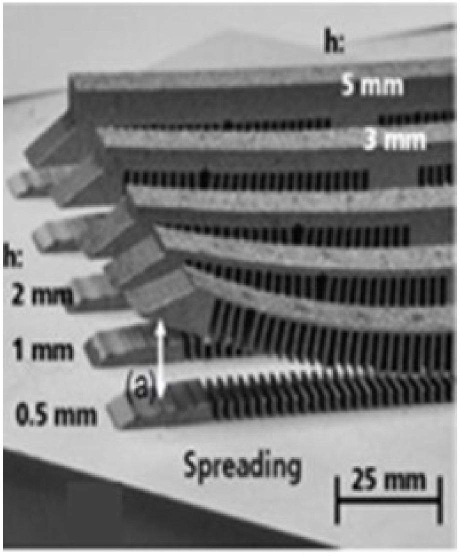

Fig. 2 DT measuring technique for RS [7].

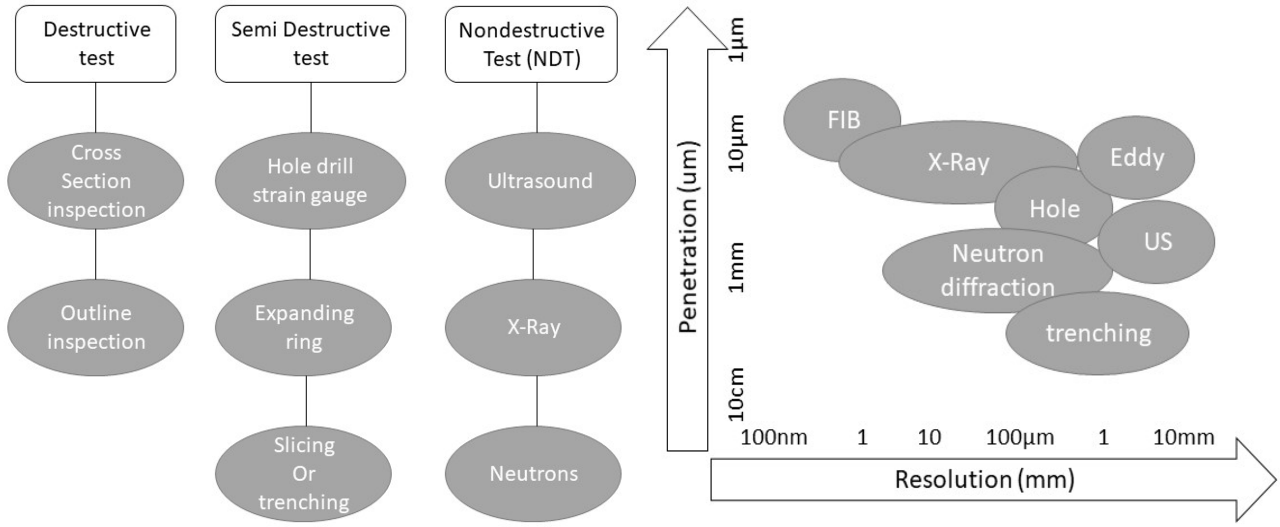

(a) (b)

Fig. 3 Penetration and spatial resolution of various RS measuring techniques. (a) destructiveness; (b) penetration vs. resolution for different testing methods.

The superposition principle used by the authors assumes that the material behaves elastically during the relaxation of RS and that the material removal does not introduce new stresses by itself to affect the measurements. These assumptions are also common to other relaxation methods like slitting and trenching. Another destructive RS measuring technique is the multi-trench method that is based on the shape of the RS profile as modified by the introduction of a trench, hole or annular groove [10]. Considering certain boundary conditions, groves shape the RS profile as modified by introduction of a transverse trench. The multi-trenching method was found to provide a simple and theoretically acceptable self-calibrating method for RS determination, particularly in the presence of unknown stress/depth distributions.

Some RS measuring techniques are indirect semi-DTs. These methods are based on the fact that stresses in the AM body are in equilibrium [3]. For instance, if the solidification of the last few layers induces tensile stresses on the surface, then it is balanced by compressive stresses deep in the bulk material. Therefore, slitting the surface layer might interfere with the stress equilibrium causing a change in state of stresses which can, in an extreme situation, cause deformation (see Fig. 1). Ti-6Al-4V produced with LMD process using bidirectional scan strategy with a spacing of 600 µm between neighboring tracks is reported by Misra and Peterson [11]. And 100 µm width and 15 mm maximum depth cut slots were made using brass wire, in 51 µm increments. The strain at each depth was measured with strain gage on the back surface opposite the cut. In this case, it has been shown that indirect RS measurements using slitting of the surface are feasible. RSs were measured in different AM build orientations, wherein a 50% change of magnitude was observed, as was expected. In the ring slitting method, a ring is cut around the point where RSs are to be determined [12]. Calibration is done using a specimen with a known residual-stress distribution. Using calibration factors, the relieved stresses of the ring, give a good estimation of the RS. It was found by Prime et al. [12] that the ring cutting technique relieved about 90% of the surface RS for a ring, whereas the hole-drilling method relieves only about 25% of the surface RS. The splitting method also mimics the deformations in material cracking due to excessive RS. A deep cut is done into a specimen and the opening or closing of the adjacent material indicates the approximate magnitude of the RS present [6]. This method is commonly used as a quick comparative test for control during material production.

A low alloy 0.2% carbon steel ring was carburized and quenched in order to induce RS through its martensitic transformation. Wang and Chou [13] used wire EDM in order to cut open the martensitic rings. Two SGs were used to measure the deflection of the ring (see Fig. 4a). The calculated residual hoop stress profile near the outer surface was compared to the X-ray diffraction NDT measurements with good agreement for the area below the surface (see Fig. 4b). The increase of the measurements profile near the surface may be due to surface decarburization or auto tempering during the air cool and is supported by the hardness measurements. The RS profile and correlation of measured and predicted values are excellent.

Another semi destructive RS measuring technique uses FIB (Focused Ion Melling Beam) (see Fig. 3) in combination with DIC (digital image correlation) technique [6]. In this technique a miniature mesh of dots is marked using the FIB Ion beam and the relaxation of stresses is measured by the DIC during trenching of the surface by the Ion beam. This technique is characterized with high resolution but also with poor penetration and it is restricted to a very small sample. A mechanical instrumented indentation technique, which is based on the experimental

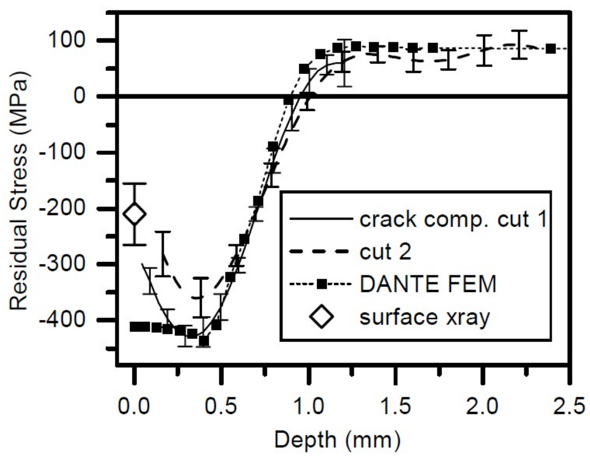

(a)

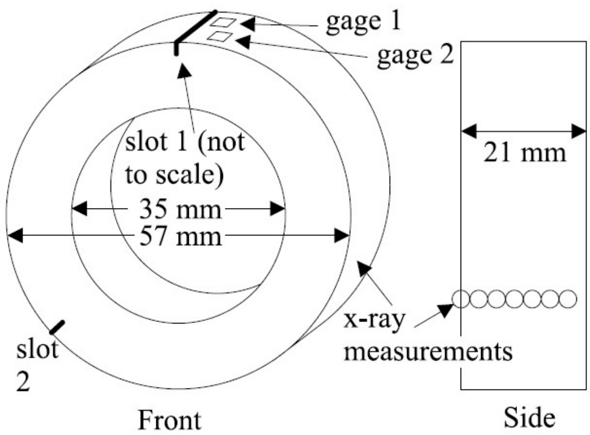

(b)

Fig. 4 Wire EDM slotting of steel ring [13]. (a) experimental setup; (b) results of RS.

correlation between the indentation characteristic and the RS was presented by Liu et al. [14]. The results show that Ti-6Al-4V parts that were produced by electron beam AM have a compressive RS in both Z and X planes. The RS measurement by Vickers micro-indentation was found to be possibly an appropriate method for the rapid evaluation of RS in microstructure scale. In order to establish a correlation between the equi-biaxial RS fields and the contact area of indentation hardness, a new indentation parameter was introduced by the authors in their model to calculate the RS for a sharp indentation image. The results show that the RS is unevenly distributed in the parts. For the Ti-6Al4V parts, the RS in both Z and X planes are compressive. However, the RS almost does not have influence on the micro-hardness of the Ti-6Al-4V. Cutting the samples of the inspected part releases some of the macro stresses and affects the integrity of the measured results.

The hole drilling technique is a very commonly used RS measuring technique. SGs (strain gauges) in 120º array are used to measure the change in surface stresses. The hole drilling measuring technique uses a highly sensitive strain rosette on the sample surface through which a hole is drilled in the rosette center [15, 16]. The material removal causes a stress relaxation in the locality around the circular hole measured by the strain rosette. The drilling operation destroys the former equilibrium state of stresses and attains a new stress equilibrium resulting in the surrounding material deformation, namely, strain relief. Therefore, it is counted as a semi DT technique. The hole drilling technique is covered by the ASTM E 837 standard [17]. Recently, a DIC optical technique has been rapidly developed and widely used to determine surface displacement in two or three dimensions. It is based on high resolution video captured during deformation. The local textured details within the sequence of images are then statistically correlated in order to determine relative displacements.

Non-destructive diffraction based methods were used to calculate the stress profile in a part that was SLM AM using different build strategies [18]. A new multi-scale approach based on the method of finite elements was developed in order to enable faster predictions of RS and distortion for AM parts [19]. Although stress and temperature of a certain point in the AM layer are affected by approximately 10 previous layers, displacement values alter until the end of the built-up process.

fs-lasers provide the capability of ablating material without significantly thermally interacting with the ablated substrate. Additionally, fs-lasers are highly energy concentrated efficient at ablating materials which further reduces the risk of thermal effects [20]. These capabilities inspire the use of the laser in a trenching operation that could possibly relieve RS without unwantedly inducing RS. It is reported in Ref. [21] that a fs-laser trenching in glass, resulted in stress-free ultra-densification, decompaction and void formation inside porous glass as a function of laser pulse energy and scanning rate. Images of the laser-decompacted regions were linearly polarized light with a crossed polarizer and an analyzer demonstrated that no collateral RSs were found. The influence of fs-laser modification on Ti-6Al4V surface fatigue was investigated by Cao et al. [21]. It was found that tensile RSs generated during surface modification using fs-laser were negligible, presenting lower values than those found on the unmodified surface.

Here a novel NDT RS measuring technique for AM was developed using a fs-laser. It could be considered semi-NDT for some applications where micron scale surface defects are inconsequential. The objective was to develop a new NDT technique using strain-gauges that are used frequently for RS measurements. A fs-laser is used to relax surface stresses by ablating a slit up to 250 μm depth without heating the slit area. The use of the fs-laser can be referred to as an NDT technique in cases where 250 μm surface scratch is not an issue. This technique can be applied to large parts with no need of cutting samples out of the whole part.

2. Experimental Procedure

2.1 Research Methodology

The state of stresses in AM is complex due to various process parameters. Each layer is melted, re-melted and annealed periodically up to approximately 15 times. Therefore, it is complicated to evaluate the RSs in full AM body. In this research, an attempt was made to replicate an SLM process in its last layer pass. A laser was applied as bead-on-plate of a single layer in variety of routes, energies and velocities, in order to evaluate the influence of varying energy depositions on RS. Two different laser routes can be seen in Fig. 5. The route with no overlap was planned as such in order to reduce annealing caused by the laser revisiting previous passes, effectively retaining RSs for measurability.

A controllable rotary welding jig device was designed and assembled in order to laser the surface of the steel rings as can be seen in Fig. 5. The use of rings was done in order to calibrate the RS measurements of direct and indirect techniques. Eventually, the ring cut technique was used in order to evaluate the influence of welding route on the RSs.

2.2 Sample Preparation

Low carbon steel samples (rings and flat bars) were annealed for 3.5 h at 850 °C in order to remove any present manufacturing stresses. An IPG's YLR-500-AC-Y14500W with 1,054 nm wavelength YAG laser was used to melt three different patterns (as shown in Fig. 6) into the samples, simulating the last laser pass of SLM built. This experiment intends to deduce correlations between laser pattern (build strategy) and RS magnitudes. The patterns contain non-lasered areas in order to preserve the surface condition of the samples to allow for proper adhesion of the SGs. The nominal chemical composition of the 1018 was: Mn0.60-0.90, C0.15-0.20, S0.05 (max) and P0.04 (max).

The T-91 sample was made with laser powder bed AM using an EOS M280 machine which had the following parameters: scan speed of 713 mm/s, laser power of 270 W, 40 μm layer thickness, and volume energy density of 78.8 J/mm^3. The scan direction was rotated by 67° for each layer pass. The build plate was 1.1730 steel 250 × 250 mm with a mini build plate on top with dimensions 117 × 117 × 12.7 mm. The sample was built with length, width and height of 12.7, 12.7 and 10.1 mm. The build strategy of the narrow side of the sample was expected to create a unidirectional RS in the longitudinal side of the sample (see Fig. 7). Powder was purchased from Carpenter Powder products (See table 1).

The Ti-6Al-4V sample was manufactured by Rotem Industries using Arcam AB, Sweden, A2X powder. The sample was EBM technique while the powder

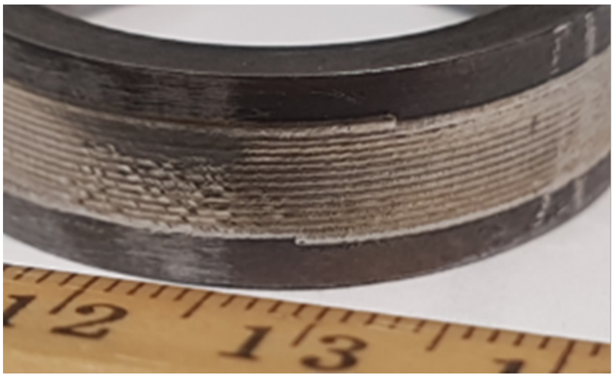

(a)

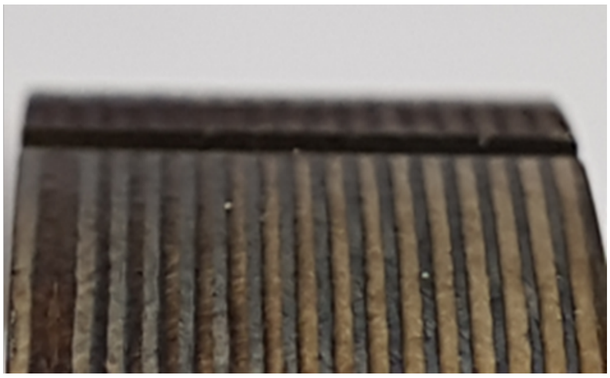

(b)

Fig. 5 250 W at 25 mm/s laser path over rings samples. (a) 50% overlap; (b) no overlap route.

Fig. 6 250 W at 25 mm/s laser build on flat 10 mm thick plate with SG spaces.

Table 1 Chemical composition of T-91 steel powder.

Element (%)	C	Mn	P	S	Cr	Mo	Ni	V	Al	Fe
ASTMA213 [20]	0.07-0.14	0.3-0.6	0.02	Max 0.02	8-9.5	0.85-1.05	Max 4.0	0.18-0.25	0.015	Bal.
This work	0.09	0.47	0.003	0.007	9.01	0.93	0.06	0.18	0.02	Bal.

Table 2 Chemical composition of Ti-6Al-4V powder.

Element (%)	Ti	Al	V	Fe	C	O	H	N
ASTMF3001 [20]	Bal.	5.5-6.5	3.5-4.5	0.25 Max	0.08 Max	0.13 Max	0.012 Max	0.05 Max
This work	Bal.	6.32	3.9	0.2	---	0.006	0.001	0.01

was spread on a pre-heated bed that was held at a temperature of 700 °C. The Arcam machine utilizes the EBM method in which the AM body is produced under a vacuum below 8×10^{-3} mbar using an electron beam focused to size of ~200 µm. An acceleration voltage of 60 kV and filament power of 1500W were applied with a scan speed of 1.5 m/s. In this process, the beam first melts powder on the circumference of the structure to be built then melts the material inside. The layer thickness is 50 µm. The original powder compositions reported by the vendors are given in Table 2.

2.3 Wiring and Mounting

SGs generate differential resistance caused by and directly proportional to the change in length of the SG miniature wires. As discussed earlier, the samples were prepared with unlayered areas for which the SGs are to be adhered to (see Fig. 6). Cyanoacrylate glue was used to adhere the 350 Ω Omega's Karma Tee Rosettes SGs (SGK-B3A-K350U-PC23-E) to the thoroughly cleaned unlayered surfaces. For each sample's experiment, two Omega's 350 Ω quarter "Wheatstone Bridge Completion Module" were used to separately detect voltages from two longitudinal and transverse positioned SGs. The bridges were powered by the Rio-Rand (LM2596) regulated voltage output of a 5.5 V Ion-metal battery. The outputs of the quarter bridges were directly connected to a data logger Omega's (DAQ-2401) with a sample rate of 1 kHz. Additionally, the samples had thermocouples drill holes which were located in parallel to surface 1 mm directly beneath the SGs. This was done in order to avoid temperature change which might directly influence the strain measurements.

2.4 Data Postprocessing and Noise Management

Both temperature of the SG's vicinity and SG (mV) were measured simultaneously during the experiments. The fs (Femto-Second) Laser, although known for not thermally interacting with materials, caused the temperature of the samples to increase slightly during the cutting process. Since the temperature directly influences strain measurements through thermal expansion, this effect was intended to be compensated for during post-processing in order to isolate strain values caused by the releasing of RSs. Furthermore, different fs-laser trenching techniques were investigated in order to achieve a 250 μm slit with minimal thermal effects.

Noise suppression was a critical operation in the data logging process. The differential voltages picked up from the SGs are on the order of millivolts which leaves the system vulnerable to the smallest EMIs (electromagnetic interferences). Precautions were taken in order to eliminate all sources of EMI and to protect the electronics from uncontrollable sources (e.g. the fs-laser). These precautions included shortening wires and avoiding power source interferences as using a battery and regulator instead of electric power supply. Other precautions that should have been taken include using shielded wires and using Faraday enclosures for sensitive components of the electronics. Although the precautions taken did help in noise suppression, the data still contained a significant amount of noise which was then smoothed out by averaging over the data points. By investigating the frequency space of the SG data using FFTs (Fast Fourier Transformations), a few peaks were identified and compensated for.

2.5 Procedure

After samples were setup and necessary precautions were taken, the samples were then positioned under the fs-laser. Two slitting strategies were adopted to relieve RSs. The first strategy involved making four parallel cuts in a sequential manner starting from 10 mm away from the SG and up to 1 mm, as shown in Fig. 7a. Between each cut, the samples were allowed to naturally cool down to room temperature and stresses released. The second strategy involved the cutting on both sides of the SG to allow for a greater amount of stresses to be relieved. It should be noted that during these experiments, it was expected to measure larger strains in the longitudinal direction (i.e. perpendicular to the laser welds) than the transverse direction.

In the case of the fs-laser trenching both sides of the SG, as seen in Fig. 7b, the slits were made sequentially. RSs were released in both longitudinal and transverse directions in a wavy manner. A possible explanation for this is that each slit released some tension on the surface causing changes in the stress balance which enhanced the compression in the other directions. The second trenching on the other side of the SG released

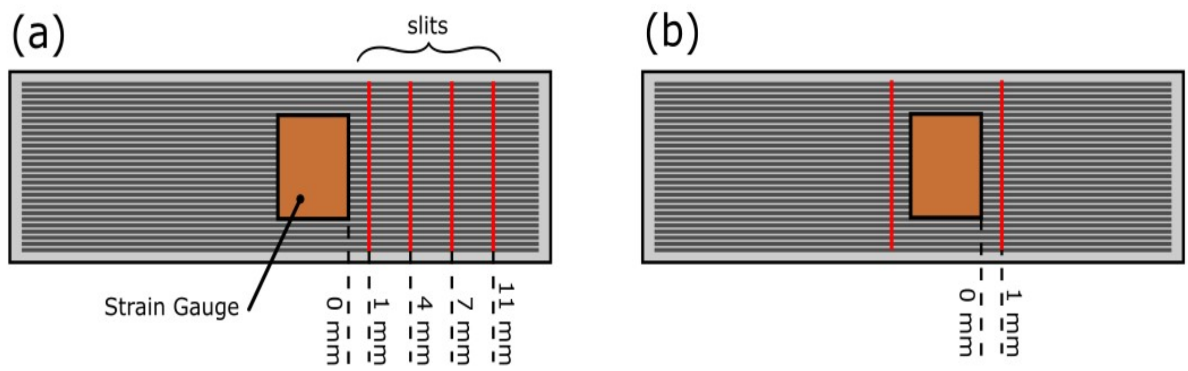

(a) (b)

Fig. 7 fs-laser slitting of low carbon steel surface lasered sample. (a) 4 trenches on the same size 11, 7, 4 and 1 mm from SG; (b) two simultaneous slitters on both SG sides.

the compression stresses back to tension. The total RSs that were released in that operation were tension as in other cases (in the order of 0.6% strain). This experiment proves that the fs-laser—SG technique presented here is sensitive enough to measure RSs and to distinguish between stress directions in the material.

3. Results and Discussion

3.1 Rings Cut Open Test

The surface lasered (see Fig. 8) low carbon steel rings were cut open using waterjet in order to avoid temperature rise and to eliminate distortion. Although the kerf of the cut was 0.1 mm, it can be seen that the elastic springing of the nonoverlap surface laser ring (Fig. 8b) was as double as the one with 50% overlap (Fig. 8a). It appears that overlap laser route annealed some 50% of the RSs as was expected. The calculation of the released elastic strain due to the cut is straight forward and can be used as a calibration technique for other non-direct techniques.

3.2 Low Carbon Steel Bars

Few series of experiments were done in variety of surface laser paths, energy’s and velocities. The strain released vs. fs-laser trench depth of a low carbon steel bar can be seen in Fig. 9. The strain is in the order of 0.2%-0.7% as was expected for this case. It can be seen that the longitudinal strain is much higher than the transverse due to the longitudinal unidirectional laser operation that was applied on the sample surface. It was found by Prime et al. [12] that about 90% of the RSs are located near the surface. This is why a 250 μm trench releases substantial amount of the RSs as were measured in this case. The results that were acquired using simulated AM process then here compared to measurements that were taken from real SLM AM Ti-6Al-4V and T-91 Ferritic steel.

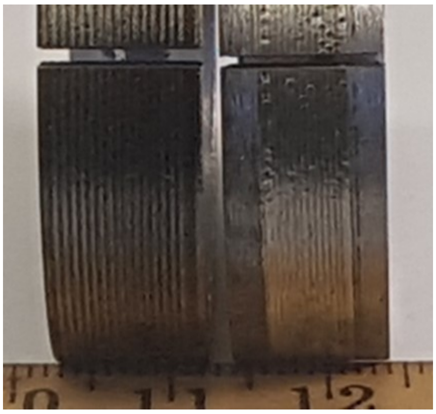

Fig. 8 Low carbon steel rings surface lasered 250 W at 25 mm/s with the same total energy. (a) no overlap; (b) 50% overlap laser route.

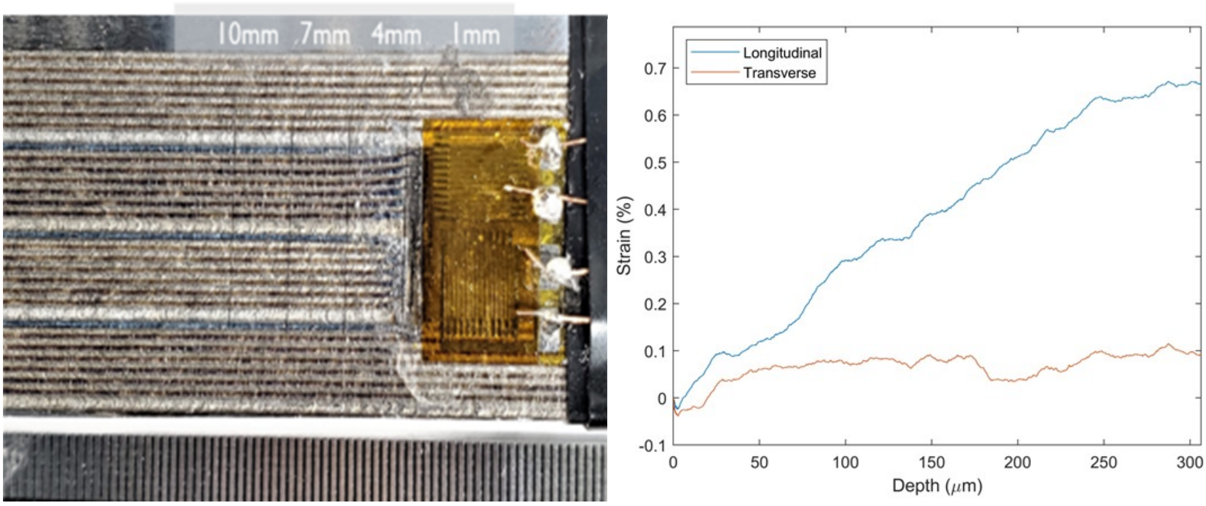

(a) (b)

Fig. 9 RS measurements in surface lasered low carbon steel 10 mm bar. (a) 4 trenches at 10, 7, 4 and 1 mm from L-T SG; (b) RSs released measurements on the 10 mm trench.

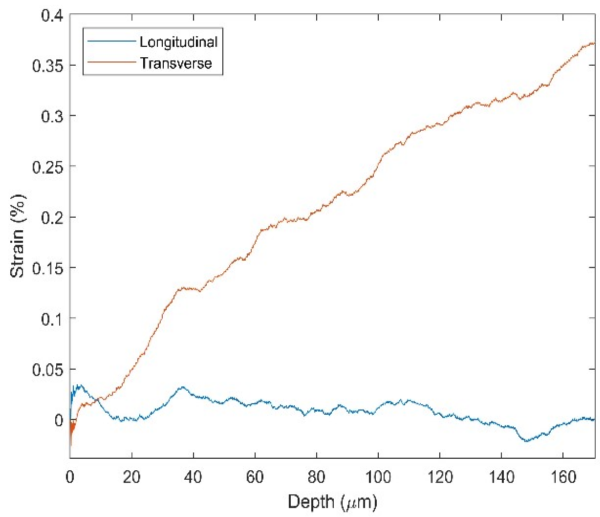

Fig. 10 RS measurements in unidirectional SLM AM T-91 ferritic steel sample. fs trench was done 4 mm from the L-T SG.

3.3 T-91 Ferritic Steel

T-91 ferritic steel was SLM AM built in a longitudinal direction route. It can also be seen in Fig. 10 that the longitudinal RSs are 5 times higher than the transverse due to the building strategy. It can also be observed that in 250 µm trance the release graph becomes asymptotic meaning most of surface RSs were released.

3.4 EMB Ti-6Al-4V RSs Measurements

The Ti-64 sample was made by electron beam powder bad system rotate 165º on the X-Y plan between each path of the EBM machine. Therefore, a homogenize state of stresses was expected in the X-Y plain. homogenize state of stresses was expected in the X-Y plain. The SG was mounted on the thinner part of the sample. It was located were the higher residual stressed were expected due to faster cooling during the build. The sample was installed with thermocouple in order to measure the temperature in the SG vicinity (see Fig. 11b). The result of fs-laser trenching in the Ti-6Al-4V can be seen in Fig. 12.

3.5 Discussion

A novel RS measurements technique is presented. The technique makes use of SGs that are in use for RS measurements for a long time and fs laser as tool for stilting the surface of the sample. Since a 250 µm trench is needed for this technique, it can be held as NDT technique for most applications. It has been shown that this technique is applicable for wrought and AM metals. It was demonstrated for steel and Ti alloys. Our results so far show that the technique parameters are similar to hole drilling technique (Fig. 3b) without the hole. This is an ongoing research and the next stage is to establish and calibrate a numerical model for wide range of AM metals and manufacturing parameters.

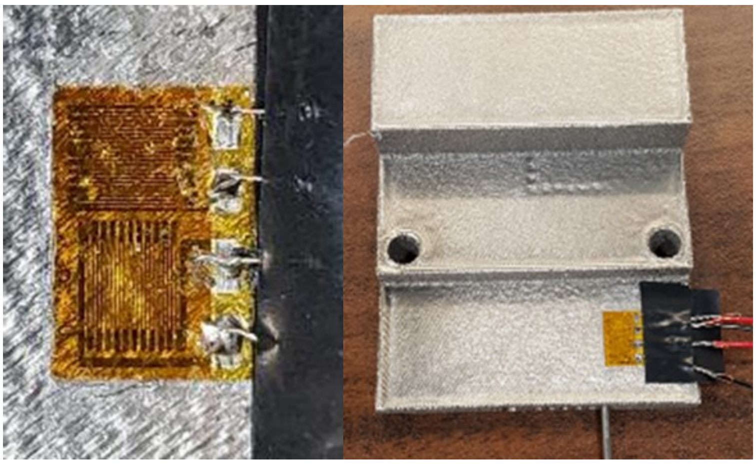

(a) (b)

Fig. 11 EMB Ti-6Al-4V. (a) L-T SG installed; (b) shielded K type thermocouple inserted.

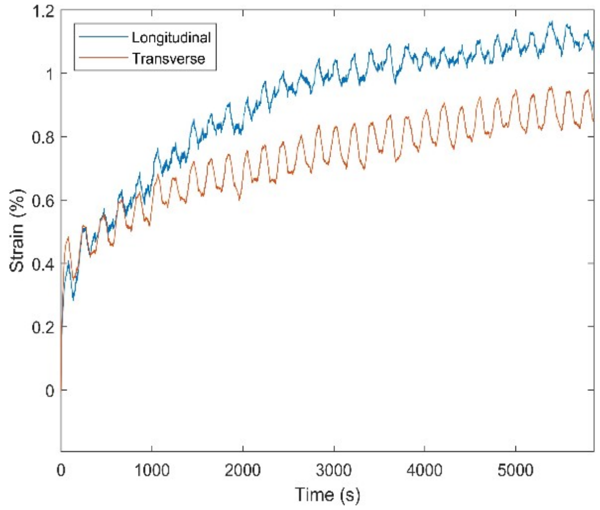

Fig. 12 RS measurements of Ti-6Al-6V AM part—the trenching of fs-laser was done in both sides of the SG.

4. Conclusions

RSs in AM processes are a consequence of some mechanisms: contraction due to volume change during the heating process and solidification. Other stresses are created due to temperature gradients or phase transformation. RS measuring techniques are categorized by destructiveness. A novel NDT RSs measuring technique was established, using SG and fs laser trenching. Laser trenching up to 250 μm depth relaxes surface stresses violating the stress balance that is measured by a bidirectional SG.

(1) It was demonstrated that this technique is sensitive enough to measure RSs in AM parts.

(2) The use of L-T type SG enables evaluation of RS in two perpendicular directions emphasizes the relationship of stresses in the part.

(3) Machine learning technique was used to support the measured results.

Acknowledgment

This project is a collaboration between UC Berkeley Nuclear and Mechanical engineering departments.

The authors acknowledge the contribution of Mr. Rony Reuven to the SGs work and to C. Lean and S. A. Maloy from LANL for providing the AM T91 sample.

References

[1] Frazier, W. E. 2014. "Metal Additive Manufacturing: A Review." *Journal of Materials Engineering and Performance* 23 (6): 1917-28

[2] Li, C., Liu, Z. Y., Fand, X. Y., and Guo, Y. B. 2019. "Residual Stresses in Metal Additive Manufacturing." In *Proceedings of the 4th Int. CIRP Conference on surface integrity (CSI 2018), Production CIRP 71*, pp. 348-53.

[3] López, C., Elías-Zúñiga, A., Jiménez, I., Martínez-Romero, O., Siller, H. R., and Diabb, J. M. 2018. "Experimental Determination of Residual Stresses Generated by Single Point Incremental Forming of AlSi10Mg Sheets Produced Using SLM Additive Manufacturing Process." *Materials* 11 (12): 2542.

[4] Gong, X., Anderson, T., and Chou, K. 2014. "Review on Powder-Based Electron Beam Additive Manufacturing Technology." *Manufacturing Rev.* 1 (2): 1-12.

[5] Heeling, T., and Wegener, K. 2018. "The Effect of Multi-beam Strategies on Selective Laser Melting of Stainless Steel 316L." *Additive Manufacturing* 22: 334-42.

[6] Schajer, G. S. 2013. *Practical Residual Stress Measurement Methods*. New York: John Wiley & Sons Ltd.

[7] Buchbinder, D., Meiners, W., Pirch, N., Wissenbach, K., and Schrage, J. 2014. "Investigation on Reducing Distortion by Preheating during Manufacture of Aluminum Components Using Selective Laser Melting." *J. Laser Appl*. 26 (1): 1-10.

[8] Rossiniab, N. S., Dassistia, M., Benyounisb, K. Y., and Olabib, A. G. 2012. "Methods of Measuring Residual Stresses in Components." *Materials & Design* 35: 572-88.

[9] Schwartz, I. F. 1994. "Multiple Trenching: A Simple Self-calibrating Method of Residual-Stress Measurement." *Experimental Mechanics* 9: 201.

[10] Strantza, M., Vrancken, B., Prime, M. B., Truman, C. E., Rombouts, M., Brown, D. W., Guillaume, P., and Van Hemelrijck, D. 2019. "Directional and Oscillating Residual Stress on the Mesoscale in Additively Manufactured Ti-6Al-4V." *Acta Materialia* 168: 299-308.

[11] Misra, A., and Peterson, H. A. 1981. "Examination of the Ring Method for Determination of Residual Stresses." In *Experimental Mechanics*, pp. 268-72.

[12] Prime, M. B., Prantil, V. C., Rangaswamy, P., and Garcia, F. P. 2000. "Residual Stress Measurement and Prediction in a Hardened Steel Ring." *Materials Science Forum* 347-349: 223-8.

[13] Wang, X., and Chou, K. 2012. "Residual Stress in Metal Parts Produced by Powder-Bed Additive Manufacturing

Processes." In *Proceedings of the 26th International Solid Freeform Fabrication Symposium*, Austin, Texas, USA, pp. 1463-74.

[14] Liu, F., Lin, X., Yang, G., Song, M., Chen, J., and Huang, W. 2011. "Microstructure and Residual Stresses of Laser Rapid Forming Inconel 718 Nickel-Base Superalloy." *Optics & Lasers Technology* 43: 208-13.

[15] Huang, X., Liu, Z., and Xie, H. 2013. "Recent Progress in Residual Stress Measurement Techniques." *Acta Mechanica Solida Sinica* 26 (6): 603-18.

[16] ASTM E837: Residual Stress Measurement by Center Hole Drilling.

[17] Robinson, J., Ashton, I., Fox, P., Jones, E., and Sutcliffe, C. 2018. "Additive Manufacturing Determination of the Effect of Scan Strategy on Residual Stress in Laser Powder Bed Fusion Additive Manufacturing." *Additive Manufacturing* 23: 13-24.

[18] Keller, N., and Ploshikhin, V. "New Method for Fast Predictions of Residual Stress and Distortion of AM Parts." In *Solid Freeform Fabrication Symposium (SFF)*, Texas, U.S.A., August 4-6, 2014.

[19] Veiko, V. P., Kudryashov, S. I., Sergeev, M. M., Zakoldaev, R. A., Danilov, P. A., Ionin, A. A., Antropova, T. V., and Anfimova, I. N. 2016. "Femtosecond Laser-Induced Stress-Free Ultra-densification inside Porous Glass." *Laser Phys. Lett.* 13: 5.

[20] ASTM A213/ASME SA213 T91: Chemical composition and mechanical properties.

[21] Santosa, A. D., Campanellia, L. C., Carvalho, P. S., da Silvaa, P., Vilarb, R., de Almeidab, M. A. M., Kuznetsovc, A., Achetec, C. A., and Bolfarinia, C. 2019. "Influence of a Femtosecond Laser Surface Modification on the Fatigue Behavior of Ti-6Al4V ELI Alloy." *Materials Research* 22 (4): e20190118. http://dx.doi.org/10.1590/1980-5373-MR-2019-0118.

[22] Cao, Y., Wang, Y., Dong, S., Yang, Y., Liang, Y., Sun, T., et al. 2007. "Residual Stresses around Femtosecond Laser Ablated Grooves in Silicon Wafer Evaluated by Nanoindentation." Presented at 3rd International Symposium on Advanced Optical Manufacturing and Testing Technologies: Large Mirrors and Telescopes, Chengdu, China.